Heterometallic Boride Clusters: Formation of Octahedral $[M_2Ru_4(CO)_{16}B]^-$ (M = Rh or Ir) and Gold(I) Phosphine Derivatives. Crystal Structures of $[N(PPh_3)_2][trans\text{-}Ir_2Ru_4(CO)_{16}B]$, $trans\text{-}[Rh_2Ru_4(CO)_{16}B\{\mu_3\text{-}AuP(C_6H_{11})_3\}]$ and $cis\text{-}[Ir_2Ru_4(CO)_{16}B\{\mu\text{-}AuP(C_6H_{11})_3\}]$ †

Jane R. Galsworthy,[a] Andrew D. Hattersley,[a] Catherine E. Housecroft,*[a,b] Arnold L. Rheingold*[c] and Anne Waller[a]

[a] *University Chemical Laboratory, Lensfield Road, Cambridge CB2 1EW, UK*
[b] *Institut fur Anorganische Chemie, Spitalstrasse 51, CH-4056 Basel, Switzerland*
[c] *Department of Chemistry, University of Delaware, Newark, DE 19716, USA*

The reaction of the butterfly cluster $[Ru_4H(CO)_{12}BH]^-$ with $[Rh_2(CO)_4Cl_2]$ led to the octahedral boride $[Rh_2Ru_4(CO)_{16}B]^-$ **1**. In solution, ^{11}B NMR spectroscopic evidence supports the presence of both *cis*- and *trans*-isomers of **1**. The *trans* form is predominant. When treated with $[AuCl\{P(C_6H_{11})_3\}]$, **1** yielded $[Rh_2Ru_4(CO)_{16}B\{AuP(C_6H_{11})_3\}]$ **3** in two isomeric forms **3a** and **3b**. Similar reactions occur with other phosphine gold(I) derivatives. The crystal structure of compound **3a** has been determined and reveals a *trans* arrangement of Rh atoms and a face capping $AuP(C_6H_{11})_3$ unit. The anion $[Ru_4H(CO)_{12}BH]^-$ reacted with $[Ir_2L_4Cl_2]$ (L = cyclooctene or L_2 = cycloocta-1,5-diene) under a stream of CO to give $[Ir_2Ru_4(CO)_{16}B]^-$ **2**; the crystal structure of **2** has been determined and confirms an octahedral metal framework with *trans* iridium atoms. Cluster **2** reacted with $[AuCl\{P(C_6H_{11})_3\}]$ to yield $[Ir_2Ru_4(CO)_{16}B\{AuP(C_6H_{11})_3\}]$ **4** and crystallographic data for **4** show that the Ir atoms are mutually *cis* in the octahedral Ir_2Ru_4 skeleton. The $AuP(C_6H_{11})_3$ unit bridges the Ir–Ir edge. In $[Ru_4H(CO)_{12}BH]^-$, the four ruthenium atoms define a butterfly framework with the boron atom lying in a semi-interstitial position. The addition of two Group 9 metal atoms to close up the metal cage to an octahedral one with an M_2Ru_4 core should initially give a *cis* isomer. In fact the *trans* isomer is observed for both **1** and **2**, although for **1** both *cis* and *trans* isomers are observed by ^{11}B NMR spectroscopy. Geometrical preferences which accompany the addition of a gold(I) phosphine fragment to anions **1** and **2** to give **3** and **4** respectively are discussed.

In recent articles we have described the formation of octahedral- and trigonal-prismatic boride clusters.[1–4] These include the homometallic cluster $[Ru_6H(CO)_{17}B]$,[1] also prepared and structurally characterized by Shore and co-workers.[5] In our previous studies, we made use of the triruthenium precursors $[Ru_3(CO)_9BH_5]$ and $[Ru_3(CO)_9(B_2H_6)]$ and their conjugate bases to prepare both homometallic hexaruthenium borides[1–3] and heterometallic systems, namely octahedral $[Rh_2Ru_4H(CO)_{16}B]$, octahedral $[Rh_2Ru_4(CO)_{16}B]^-$ and the capped double-trigonal prismatic $[Rh_3Ru_6(CO)_{23}B_2]^-$.[4] Fehlner and co-workers[6–8] have successfully utilized the ferraborane anion $[Fe_4H(CO)_{12}BH]^-$ in reaction with $[Rh_2(CO)_4Cl_2]$ to produce the heterometallic boride cluster *trans*-$[Fe_4Rh_2(CO)_{16}B]^-$. During this reaction, ^{11}B NMR spectroscopic studies have confirmed the formation of an intermediate M_5 cluster species followed by the generation of an initial M_6B product, defined from the spectroscopic data to be *cis*-$[Fe_4Rh_2(CO)_{16}B]^-$.[6–8] The kinetics of the cage isomerism to *trans*-$[Fe_4Rh_2(CO)_{16}B]^-$ has been investigated in detail.[7,8] As Fehlner points out, the isomerism has an isolobal counterpart in the conversion of the carbaborane 1,2-$C_2B_4H_6$ to 1,6-$C_2B_4H_6$.

In the report of the preparation of $[Rh_2Ru_4(CO)_{16}B]^-$ **1** from $[Ru_3(CO)_9BH_4]^-$,[4] we stated that this anion could also be produced in good yield from the reaction of $[Ru_4H(CO)_{12}BH]^-$ with $[Rh_2(CO)_4Cl_2]$.[9] Here this work is reported in full and the results compared with those obtained for the introduction of iridium into the cluster framework. The preparative procedure for **1** follows that reported by Fehlner and co-workers[6,8] for $[Fe_4Rh_2(CO)_{16}B]^-$, but we notice some significant differences with regard to the relative preferences for *cis*- and *trans*-cage geometries when we compare the results for the iron- and ruthenium-containing and the rhodium- *versus* iridium-containing metal frameworks. Also reported here are the reactions of the anionic borides with $[AuCl\{P(C_6H_{11})_3\}]$ and $[AuCl(PPh_3)]$, and the observation that a *cis*-Ru_4Ir_2 cage can be isolated in the form of a gold(I) phosphine derivative.

Experimental

General.—Fourier-transform NMR spectra were recorded on a Bruker WM 250 or AM 400 spectrometer; ^1H and ^{13}C shifts are reported with respect to δ 0 for $SiMe_4$, ^{11}B with respect to δ 0 for $BF_3{\cdot}OEt_2$ and ^{31}P with respect to δ 0 for H_3PO_4. All downfield chemical shifts are positive. Infrared spectra were recorded on a Perkin-Elmer FT 1710 spectrophotometer; FAB (fast atom bombardment) mass spectra on Kratos instruments with 3-nitrobenzyl alcohol as matrix.

All reactions were carried out under argon by using standard Schlenk techniques. Solvents were dried over suitable reagents and freshly distilled under N_2 before use. Separations were carried out by thin-layer plate chromatography with Kieselgel 60-PF-254 (Merck). The compounds $[Rh_2(CO)_4Cl_2]$ and

† *Supplementary data available:* see Instructions for Authors, *J. Chem. Soc., Dalton Trans.*, 1995, Issue 1, pp. xxv–xxx.

$[Ir_2L_4Cl_2]$ [L = cyclooctene or L_2 = cycloocta-1,5-diene (cod)] were used as received (Aldrich), whereas $[N(PPh_3)_2][Ru_3(CO)_9BH_4]$,[1] $[N(PPh_3)_2][Ru_3(CO)_9(B_2H_5)]$[3] and $[Ru_4H(CO)_{12}BH_2]$[10] were prepared as previously described. Yields are with respect to the starting ruthenium cluster for the preparations of **1** and **2**, or with respect to **1** and **2** for **3** and **4**, respectively.

Preparation of the $[N(PPh_3)_2]^+$ *Salt of* $[Rh_2Ru_4(CO)_{16}B]^-$ **1**.—In a typical reaction, $[Ru_4H(CO)_{12}BH_2]$ (80 mg, 0.11 mmol) was dissolved in CH_2Cl_2 (10 cm^3) and $[N(PPh_3)_2][O_2CMe]$ (66 mg, 0.11 mmol) added. The solution was stirred at room temperature for 5 min to give an orange solution. The approximately quantitative formation of $[N(PPh_3)_2][Ru_4H(CO)_{12}BH]$[10] was confirmed by IR spectroscopy. To this solution *in situ* was added $[Rh_2(CO)_4Cl_2]$ (42 mg, 0.11 mmol) and the mixture stirred at room temperature for 30 min during which time it became brown. The products were separated by TLC (3:1 CH_2Cl_2–hexane). Two initial yellow fractions were identified as $[Ru_4H(CO)_{12}BH_2]$[10,11] and $[Ru_4H_4(CO)_{12}]$.[12] The compound $[N(PPh_3)_2][Rh_2Ru_4(CO)_{16}B]$ (≈50%) was collected as a brown fraction ($R_f \approx 0.5$) and identified from spectroscopic and mass spectrometric data previously reported.[4] Additionally, note that in $[^2H_8]$thf (thf = tetrahydrofuran), the triplet signal in the ^{11}B NMR spectrum for $[Rh_2Ru_4(CO)_{16}B]^-$ **1** is at δ +197.3 (this work) compared to δ +193.4 in $CDCl_3$ (ref. 4).

Reaction of $[N(PPh_3)_2][Ru_4H(CO)_{12}BH]$ *with* $[Ir_2L_4Cl_2]$ (L = *cyclooctene or* L_2 = *cod*).—The same procedure was followed for both starting iridium complexes. The distribution of products was virtually independent of the iridium precursor. The method is given here for $[Ir_2L_4Cl_2]$ (L = cyclooctene).

The compound $[Ir_2L_4Cl_2]$ (L = cyclooctene) (80 mg, 0.09 mmol) was dissolved in CH_2Cl_2 (10 cm^3) and a steady stream of CO (1 atm) bubbled through the solution for 1 h. A black precipitate formed in the orange solution almost immediately. To this mixture was added a solution of $[N(PPh_3)_2][Ru_4H(CO)_{12}BH]$ (120 mg, 0.09 mmol) in CH_2Cl_2 (10 cm^3) and the stream of CO continued for a further 1 h. A red-brown solution was collected after filtering the reaction mixture through a medium-grade sinter. The solvent was reduced and the products were separated by TLC, eluting with CH_2Cl_2–hexane (2:1). An initial yellow fraction was identified as $[Ru_4H(CO)_{12}BH_2]$.[10,11] The second fraction was orange ($R_f \approx 0.45$) and has eluded characterization. The major product ($R_f \approx 0.4$, yield ≈ 60%) was the orange $[N(PPh_3)_2]^+$ salt of $[Ir_2Ru_4(CO)_{16}B]^-$ **2**: 400 MHz ^1H NMR ($CDCl_3$, 298 K), δ 7.7–7.5 (m, Ph); 128 MHz ^{11}B NMR ($CDCl_3$, 298 K), δ +199.1; IR (CH_2Cl_2, cm^{-1}) ν_{CO} 2024vs, 1996w (sh), 1825w; FAB mass spectrum, *m/z* 1250 (P^-) (Calc. for $^{11}B_1{}^{12}C_{16}{}^{192}Ir_2{}^{16}O_{16}{}^{101}Ru_4$ 1247).

Reaction of $[N(PPh_3)_2][Rh_2Ru_4(CO)_{16}B]$ *with* $[AuCl\{P(C_6H_{11})_3\}]$.—The compound $[N(PPh_3)_2][Rh_2Ru_4(CO)_{16}B]$ (20 mg, 0.012 mmol) was dissolved in CH_2Cl_2 (3 cm^3) and an excess (≈3 fold) of $[AuCl\{P(C_6H_{11})_3\}]$ added. The reaction mixture was stirred for 5 min and products separated by TLC (2:1 hexane–CH_2Cl_2). Two fractions were observed: a brown band ($R_f \approx 0.8$) and a dark green band ($R_f \approx 0.7$). In CH_2Cl_2 solution, the brown product rapidly converted to the green product and spectroscopic data indicated that the two compounds were isomers, **3a** (green) and **3b** (brown). The yield of $[Rh_2Ru_4(CO)_{16}B\{AuP(C_6H_{11})_3\}]$ **3a** from the initial separation was ≈70%.

Compound **3a**: 400 MHz ^1H NMR ($CDCl_3$, 298 K), δ 2.5–1.5 (m, C_6H_{11}); 128 MHz ^{11}B NMR ($CDCl_3$, 298 K), δ +196.2 (br); 162 MHz ^{31}P NMR ($CDCl_3$, 298 K) δ +85.8 (s); ^{13}C NMR ($CDCl_3$, 298 K) δ +200.4 (t, J_{RhC} = 11 Hz), see text; IR (CH_2Cl_2, cm^{-1}) ν_{CO} 2083w, 2047vs, 2035m (sh), 1998m, 1881w, 1857w; FAB mass spectrum, *m/z* 1549 (P^-) with intense fragmentation envelope at 1069 [P^- − $AuP(C_6H_{11})_3$] (Calc. for $^{12}C_{34}{}^1H_{33}{}^{197}Au_1{}^{11}B_1{}^{16}O_{16}{}^{31}P_1{}^{103}Rh_2{}^{101}Ru_4$ 1546). For **3b**, see text.

Reaction of $[N(PPh_3)_2][Rh_2Ru_4(CO)_{16}B]$ *with* $[AuCl(PPh_3)]$.—The reaction was carried out in an analogous manner and on the same scale as that with $[AuCl\{P(C_6H_{11})_3\}]$. Two isomers of $[Rh_2Ru_4(CO)_{16}B\{Au(PPh_3)\}]$ were observed; the green isomer could be isolated but the brown converted to the green in solution. Green isomer of $[Rh_2Ru_4(CO)_{16}B\{Au(PPh_3)\}]$: 400 MHz ^1H NMR ($CDCl_3$, 298 K), δ 7.5–7.7 (m, Ph); 128 MHz ^{11}B NMR ($CDCl_3$, 298 K), δ +196.0 (br); 162 MHz ^{31}P NMR ($CDCl_3$, 298 K), δ +69.5 (s); IR (CH_2Cl_2, cm^{-1}) ν_{CO} 2085w, 2048vs, 2035m (sh), 2000m, 1993w (sh), 1881w, 1857w; FAB mass spectrum, *m/z* 1532 (P^-) with intense fragmentation envelope at 1069 (P^- − $AuPPh_3$) (Calc. for $^{12}C_{34}{}^1H_{15}{}^{197}Au_1{}^{11}B_1{}^{16}O_{16}{}^{31}P_1{}^{103}Rh_2{}^{101}Ru_4$ 1528). For brown isomer, see text.

Reaction of $[N(PPh_3)_2][Rh_2Ru_4(CO)_{16}B]$ *with* $[AuCl\{P(C_6H_4Me\text{-}2)_3\}]$.—The reaction was carried out in an analogous manner and on the same scale as that with $[AuCl\{P(C_6H_{11})_3\}]$. Only one product (green) was isolated. $[Rh_2Ru_4(CO)_{16}B\{AuP(C_6H_4Me\text{-}2)_3\}]$: 400 MHz ^1H NMR ($CDCl_3$, 298 K), δ 7.2–7.6 (m, 12 H, aryl), 2.47 (s, 9 H, Me); 128 MHz ^{11}B NMR ($CDCl_3$, 298 K), δ +195.8 (br); 162 MHz ^{31}P NMR ($CDCl_3$, 298 K), δ +58.8 (s); IR (CH_2Cl_2, cm^{-1}) ν_{CO} 2083w, 2068w, 2045vs, 2035m (sh), 2000m, 1881vw, 1857w; FAB mass spectrum, *m/z* 1570 (P^+) with intense fragmentation envelope at 1069 [P^+ − $AuP(C_6H_4Me\text{-}2)_3$] (Calc. for $^{12}C_{37}{}^1H_{21}{}^{197}Au_1{}^{11}B_1{}^{16}O_{16}{}^{31}P_1{}^{103}Rh_2{}^{101}Ru_4$ 1570).

Reaction of $[N(PPh_3)_2][Ir_2Ru_4(CO)_{16}B]$ *with* $[AuCl\{P(C_6H_{11})_3\}]$.—The compound $[N(PPh_3)_2][Ir_2Ru_4(CO)_{16}B]$ (80 mg, 0.04 mmol) was dissolved in CH_2Cl_2 (5 cm^3) and $[AuCl\{P(C_6H_{11})_3\}]$ (51 mg, 0.10 mmol) added. The reaction mixture was stirred for 2 h and products separated by TLC (2:1 hexane–CH_2Cl_2). One fraction, $[Ir_2Ru_4(CO)_{16}B\{AuP(C_6H_{11})_3\}]$ **4**, was collected as an orange-red band ($R_f \approx 0.8$) in typically 60% yield: 400 MHz ^1H NMR ($CDCl_3$, 298 K), δ 2.3–1.4 (m, C_6H_{11}); 128 MHz ^{11}B NMR ($CDCl_3$, 298 K), δ +199.7; 162 MHz ^{31}P NMR ($CDCl_3$, 298 K), δ +94.3 (s); IR (CH_2Cl_2, cm^{-1}) ν_{CO} 2089w, 2061vs, 2050s, 2029vs, 2007m; FIB mass spectrum, *m/z* 1723 (P^+) with 9 CO losses (Calc. for $^{12}C_{34}{}^1H_{33}{}^{197}Au_1{}^{11}B_1{}^{16}O_{16}{}^{31}P_1{}^{192}Ir_2{}^{101}Ru_4$ 1724).

Reaction of $[N(PPh_3)_2][Ir_2Ru_4(CO)_{16}B]$ *with* $[AuCl(PPh_3)]$.—The compound $[N(PPh_3)_2][Ir_2Ru_4(CO)_{16}B]$ (80 mg, 0.04 mmol) was dissolved in CH_2Cl_2 (5 cm^3) and $[AuCl(PPh_3)]$ (49 mg, 0.10 mmol) added. The reaction mixture was stirred for 2 h and products separated by TLC (2:1 hexane–CH_2Cl_2). One fraction, $[Ir_2Ru_4(CO)_{16}B\{Au(PPh_3)\}]$ **5**, was collected as an orange band ($R_f \approx 0.7$) in typically 60% yield; 400 MHz ^1H NMR ($CDCl_3$, 298 K), δ 7.7–7.4 (m, Ph); 128 MHz ^{11}B NMR ($CDCl_3$, 298 K), δ +199.4; 162 MHz ^{31}P NMR ($CDCl_3$, 298 K), δ +65.9 (s); IR (CH_2Cl_2, cm^{-1}) ν_{CO} 2089w, 2061vs, 2049s, 2028vs, 2006m; FIB mass spectrum, *m/z* 1707 (P^+) with 8 CO losses (Calc. for $^{12}C_{34}{}^1H_{15}{}^{197}Au_1{}^{11}B_1{}^{16}O_{16}{}^{31}P_1{}^{192}Ir_2{}^{101}Ru_4$ 1706).

Crystal Structure Determinations.—Crystallographic data for $[N(PPh_3)_2][Ir_2Ru_4(CO)_{16}B]$, **3a** and **4** are collected in Table 1. Crystals (all deep red) were mounted on fine glass fibres with epoxy cement. Photographic evidence showed that all possessed 2/*m* Laue symmetry. For $[N(PPh_3)_2][Ir_2Ru_4(CO)_{16}B]$ and **3a**, the space groups were uniquely determined by the systematic absences in the diffraction data. For **4**, the absences indicated either *Cc* or *C*2/*c*. Molecular symmetry and lattice alignment allowed only the non-centrosymmetric alternative which was supported by the results of the refinement. Semiempirical corrections for absorption were

Table 1 Crystallographic data for $[N(PPh_3)_2][Ir_2Ru_4(CO)_{16}B]$, **3a** and **4**

	$[N(PPh_3)_2][Ir_2Ru_4(CO)_{16}B]$	**3a**	**4**
Formula	$C_{52}H_{30}BIr_2NO_{16}P_2Ru_4$	$C_{34}H_{33}AuBO_{16}PRh_2Ru_4$	$C_{34}H_{33}AuBIr_2O_{17}PRu_4$
M	1786.3	1546.4	1741.0
Crystal system	Monoclinic	Monoclinic	Monoclinic
Crystal size/mm	0.60 × 0.28 × 0.56	0.20 × 0.30 × 0.40	0.08 × 0.32 × 0.41
Space group	$P2_1/n$	$P2_1/c$	Cc
a/Å	16.490(4)	14.479(5)	26.850(8)
b/Å	10.400(2)	16.852(5)	9.525(2)
c/Å	33.290(10)	18.371(5)	17.683(3)
β/°	95.52(2)	101.85(3)	101.90(2)
U/Å^3	5679(2)	4387(2)	4425(2)
Z	4	4	4
T/K	293	293	296
D_c/g cm^{-3}	2.092	2.341	2.613
μ(Mo-Kα)/cm^{-1}	58.31	55.06	107.20
Reflections collected	9178	10 067	4862
Independent reflections	9008	9786	4267
Observed reflections ($5\sigma F_o$)	2994	4448	3600
$F(000)$	3376	2920	1588
x in $w^{-1} = \sigma^2(F) + xF^2$	0.0015	0.0010	0.0015
R, R'	0.0589, 0.0693	0.0501, 0.0563	0.0528, 0.0750
Largest and mean Δ/σ	0.518, 0.022	0.001, 0.000	0.233, 0.014
Largest difference peak/e Å^{-3}	1.68	1.92	2.52
Largest difference hole/e Å^{-3}	−1.13	−1.21	−2.31

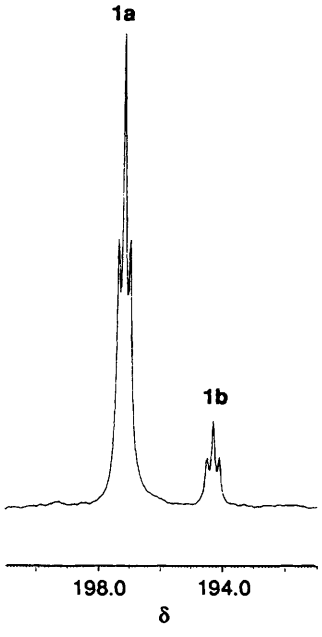

Fig. 1 The 128 MHz ^{11}B NMR spectrum ([$^2H_8$]thf, 298 K) of the *trans* (**1a**) and *cis* (**1b**) isomers of $[Rh_2Ru_4(CO)_{16}B]^-$. The solution contains the $[N(PPh_3)_2]^+$ salts of the anions

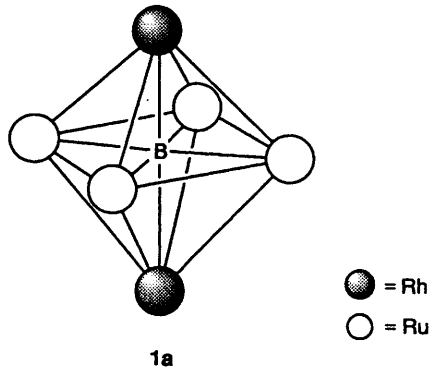

applied using 216 ψ-scan data. The structures were solved by direct methods.

In $[N(PPh_3)_2][Ir_2Ru_4(CO)_{16}B]$, a second orientation of the octahedral cluster was found at an occupancy of 8%. Only the Ir locations could be sufficiently well resolved to allow refinement. The occupancy of the two Ir positions was constrained to unity; all other atoms were refined at full occupancy. The incorporation of the partial disorder model reduced the R factor from 0.0633 to 0.0589. The limited data available for $[N(PPh_3)_2][Ir_2Ru_4(CO)_{16}B]$ required that only the atoms with $Z \geqslant 8$ be refined anisotropically. For **3a**, all the non-hydrogen atoms were refined anisotropically. For **4**, a stand-alone peak, O(100), in a late difference map had a density appropriate for oxygen and was refined as such; no chemical identity was assigned. The intensive properties for this structure include the O atom. Only those atoms with $Z \geqslant 8$ were refined anisotropically. In all the structures the hydrogen atoms were idealized.

All computations used the SHELXTL-PC software.[13] Atomic coordinates for anion **2** and for compounds **3a** and **4** are given in Tables 2, 4 and 6, respectively.

Additional material available from the Cambridge Crystallographic Data Centre comprises H-atom coordinates, thermal parameters and remaining bond lengths and angles.

Results and Discussion

Anion **1**.—The reaction of $[Ru_4H(CO)_{12}BH]^-$ with $[Rh_2(CO)_4Cl_2]$ gives the cluster anion $[Rh_2Ru_4(CO)_{16}B]^-$ **1** which has been isolated in good yield as its $[N(PPh_3)_2]^+$ salt. We have previously prepared $[N(PPh_3)_2][Rh_2Ru_4(CO)_{16}B]$ from the reaction of $[N(PPh_3)_2][Ru_3(CO)_9BH_4]$ with $[Rh_2(CO)_4Cl_2]$ and characterized it both spectroscopically and crystallographically.[4]

The ^{11}B NMR signal for anion **1** is a characteristic triplet (δ +193.4 in $CDCl_3$) with the ^{103}Rh–^{11}B spin–spin coupling of 26 Hz confirming the presence of two rhodium nuclei in the immediate proximity of the boron nucleus. We have now observed that the shift of the signal is dependent upon solvent and in [$^2H_8$]thf the resonance is at δ +197.3. In addition to the data previously reported for **1**, we have observed that in samples

of **1** produced in the reaction of $[N(PPh_3)_2][Ru_4H(CO)_{12}BH]$ with $[Rh_2(CO)_4Cl_2]$, a second triplet at δ +194.2 (Fig. 1) is present in the ^{11}B NMR spectrum in $[^2H_8]$thf. Its presence is apparent in concentrated solutions of **1**. We assign these two triplets to two isomers of **1** in which the rhodium atoms are mutually *trans* (**1a**) or *cis* (**1b**) within the octahedral metal skeleton. Justification for this is given below.

Crystallographic data have established that the Rh_2Ru_4 core of anion **1a** as its $[N(PPh_3)_2]^+$ salt has the two rhodium atoms in a *trans* arrangement.[4] The solution properties of the $[N(PPh_3)_2]^+$ salt **1a** formed from the reaction of $[Ru_4H(CO)_{12}BH]^-$ with $[Rh_2(CO)_4Cl_2]$ replicate those of the samples prepared from $[N(PPh_3)_2][Ru_3(CO)_9BH_4]$. We therefore conclude that, providing the solid-state structure is representative of the bulk sample, then **1a** prepared from $[Ru_4H(CO)_{12}BH]^-$ with $[Rh_2(CO)_4Cl_2]$ is also the *trans* isomer. It is reasonable that the minor component **1b** in solutions containing **1a** is the *cis* isomer. Further evidence for this proposal comes from the products of the reactions with gold(I) phosphines (see later).

Fehlner and co-workers[6,8] have illustrated that the *cis*- and *trans*-isomers of $[Fe_4Rh_2(CO)_{16}B]^-$ exhibit rather different ^{11}B NMR spectral shifts (*cis* isomer δ 205; *trans* isomer δ 211). The pattern is that the more downfield resonance is due to the *trans* species. This trend is consistent with our proposal for the case of the isomers of anion **1**. When the reaction mixture of $[Fe_4H(CO)_{12}BH]^-$ and $[Rh_2(CO)_4Cl_2]$ was monitored by ^{11}B NMR spectroscopy, the initial formation of *cis*-$[Fe_4Rh_2(CO)_{16}B]^-$ and its conversion to *trans*-$[Fe_4Rh_2(CO)_{16}B]^-$ could be observed; the production of *cis*-$[Fe_4Rh_2(CO)_{16}B]^-$ was preceded by the formation of a short-lived M_5B intermediate.[6,8] In the case of the reaction of $[Ru_4H(CO)_{12}BH]^-$ with $[Rh_2(CO)_4Cl_2]$, ^{11}B NMR spectral data suggest that both *cis*- and *trans*-$[Rh_2Ru_4(CO)_{16}B]^-$ are formed, but we have not been able to monitor the conversion of one to another. In solution, the relative proportions of isomers **1a** and **1b** were monitored over a period of 9 d after the reaction of $[N(PPh_3)_2][Ru_4H(CO)_{12}BH]$ with $[Rh_2(CO)_4Cl_2]$. There was no change in peak intensity in the ^{11}B NMR spectrum. The *trans* isomer always predominates in solution as shown in Fig. 1.

Anion **2**.—The formation of an iridium analogue of **1a** can be achieved by reacting $[Ru_4H(CO)_{12}BH]^-$ with $[Ir_2L_4Cl_2]$ (L = cyclooctene or L_2 = cod) under a stream of carbon monoxide. The product $[Ir_2Ru_4(CO)_{16}B]^-$ **2** has been isolated as the $[N(PPh_3)_2]^+$ salt. In solution, anion **2** exhibits just one signal in its ^{11}B NMR spectrum, a singlet at δ +199.1 in keeping with the boron residing in a fully interstitial environment.

A red, single crystal of $[N(PPh_3)_2][Ir_2Ru_4(CO)_{16}B]$ suitable for X-ray analysis was grown from a CH_2Cl_2 solution layered with hexane. The molecular structure of anion **2** is shown in Fig. 2 and selected bond distances and angles are given in Table 3. The Ir_2Ru_4 cage is octahedral, a geometry which is consistent with the 86 electron count of **2**. The two iridium atoms are

Table 2 Atomic coordinates ($\times 10^4$) for $[N(PPh_3)_2][Ir_2Ru_4(CO)_{16}B]$

Atom	x	y	z	Atom	x	y	z
Ir(1)	6 333.5(8)	8 492(2)	1 531.0(5)	C(15)	6 859(27)	10 661(48)	1 545(15)
Ir(2)	8 091.5(8)	7 730(2)	763.2(5)	C(16)	7 412(19)	11 383(34)	789(11)
Ir(1A)	6 744(35)	9 446(60)	795(18)	N	7 833(12)	14 220(21)	−1 572(7)
Ir(2A)	7 772(38)	6 601(62)	1 485(20)	C(21)	8 568(20)	12 950(35)	−524(10)
Ru(1)	8 011(1)	7 731(3)	1 657.3(8)	C(22)	8 634(20)	11 858(33)	−296(10)
Ru(2)	6 920(2)	6 138(2)	1 111.3(8)	C(23)	7 958(20)	10 984(36)	−299(10)
Ru(3)	6 351(1)	8 445(3)	611.5(8)	C(24)	7 232(19)	11 240(32)	−529(10)
Ru(4)	7 551(1)	10 014(2)	1 162.0(8)	C(25)	7 207(18)	12 388(30)	−777(9)
P(1)	7 780(4)	14 551(7)	−1 108(2)	C(26)	7 832(14)	13 183(24)	−778(8)
P(2)	7 811(4)	13 096(7)	−1 880(2)	C(31)	6 481(16)	16 168(27)	−1 349(9)
O(1)	6 370(14)	8 158(24)	2 450(7)	C(32)	5 782(19)	16 860(32)	−1 299(11)
O(2)	4 555(17)	9 198(40)	1 324(10)	C(33)	5 475(18)	16 737(30)	−907(10)
O(3)	8 660(14)	5 299(23)	371(7)	C(34)	5 792(17)	15 978(28)	−620(10)
O(4)	9 373(13)	9 535(23)	486(8)	C(35)	6 503(16)	15 278(27)	−672(9)
O(5)	9 692(12)	6 862(23)	1 482(7)	C(36)	6 848(15)	15 390(26)	−1 042(9)
O(6)	8 652(14)	9 645(25)	2 301(7)	C(41)	8 604(17)	16 421(29)	−598(9)
O(7)	7 854(18)	5 658(29)	2 278(8)	C(42)	9 235(20)	17 149(34)	−488(11)
O(8)	5 606(22)	5 217(35)	1 600(10)	C(43)	9 881(20)	17 216(32)	−690(10)
O(9)	6 274(15)	4 701(23)	364(8)	C(44)	9 918(18)	16 474(29)	−1 036(10)
O(10)	8 066(16)	3 968(25)	1 396(8)	C(45)	9 266(16)	15 633(27)	−1 161(9)
O(11)	5 551(19)	10 949(28)	354(10)	C(46)	8 609(16)	15 623(27)	−939(9)
O(12)	4 832(14)	6 971(26)	388(7)	C(51)	8 529(16)	11 166(27)	−1 431(8)
O(13)	7 051(15)	8 150(23)	−154(7)	C(52)	8 552(19)	9 947(32)	−1 249(10)
O(14)	9 207(16)	11 111(31)	1 455(10)	C(53)	7 889(20)	9 154(36)	−1 279(10)
O(15)	6 551(19)	11 609(25)	1 697(10)	C(54)	7 213(17)	9 487(30)	−1 531(9)
O(16)	7 356(20)	12 136(27)	542(8)	C(55)	7 164(19)	10 684(30)	−1 733(10)
C(1)	6 346(19)	8 319(33)	2 116(11)	C(56)	7 854(14)	11 515(25)	−1 676(8)
C(2)	5 225(25)	8 863(40)	1 401(12)	C(61)	8 958(15)	12 159(28)	−2 344(8)
C(3)	8 457(20)	6 136(35)	542(11)	C(62)	9 634(19)	12 327(33)	−2 579(10)
C(4)	8 930(19)	8 915(33)	582(10)	C(63)	9 925(19)	13 523(32)	−2 657(10)
C(5)	9 054(24)	7 224(37)	1 489(11)	C(64)	9 599(17)	14 596(32)	−2 483(9)
C(6)	8 399(19)	8 901(34)	2 074(10)	C(65)	8 952(16)	14 425(29)	−2 248(9)
C(7)	7 920(22)	6 409(40)	2 048(13)	C(66)	8 664(13)	13 218(24)	−2 185(8)
C(8)	6 071(26)	5 738(43)	1 442(14)	C(71)	6 185(17)	13 547(28)	−2 071(10)
C(9)	6 527(19)	5 263(35)	643(11)	C(72)	5 444(19)	13 564(31)	−2 318(10)
C(10)	7 661(20)	4 751(37)	1 294(10)	C(73)	5 444(21)	13 254(32)	−2 709(11)
C(11)	5 879(24)	10 016(43)	455(12)	C(74)	6 137(18)	12 954(29)	−2 901(10)
C(12)	5 395(21)	7 536(32)	494(10)	C(75)	6 863(17)	12 891(28)	−2 626(9)
C(13)	6 909(26)	8 131(45)	178(15)	C(76)	6 887(15)	13 211(26)	−2 232(9)
C(14)	8 541(23)	10 758(37)	1 385(11)	B	7 193(17)	8 093(30)	1 156(10)

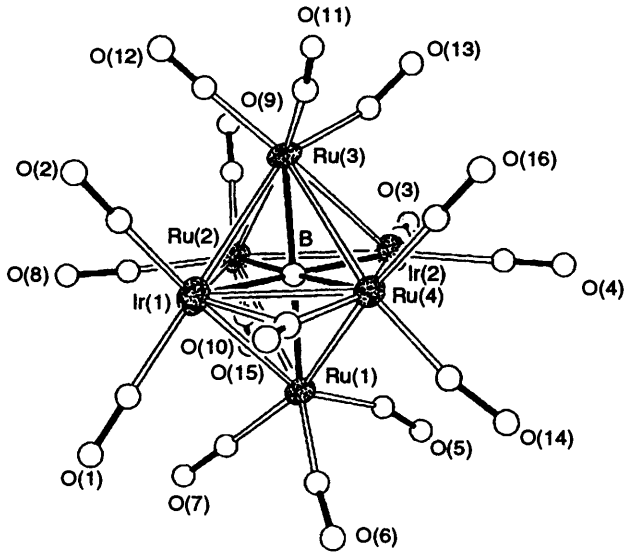

Fig. 2 Molecular structure of $[Ir_2Ru_4(CO)_{16}B]^-$ **2**

Table 3 Selected bond distances (Å) and angles (°) for anion **2**

Ir(1)–Ru(1)	2.870(3)	Ir(1)–Ru(2)	3.024(3)
Ir(1)–Ru(3)	2.898(3)	Ir(1)–Ru(4)	2.919(3)
Ir(2)–Ru(1)	2.992(3)	Ir(2)–Ru(2)	2.872(3)
Ir(2)–Ru(3)	2.953(3)	Ir(2)–Ru(4)	2.903(3)
Ru(1)–Ru(2)	2.943(3)	Ru(2)–Ru(3)	2.934(4)
Ru(3)–Ru(4)	2.953(3)	Ru(1)–Ru(4)	2.948(4)
Ru(1)–B	2.08(3)	Ru(2)–B	2.09(3)
Ru(3)–B	2.08(3)	Ru(4)–B	2.08(3)
Ir(1)–B	2.02(3)	Ir(2)–B	2.10(3)
Ru(1)–Ir(1)–Ru(3)	92.3(1)	Ru(2)–Ir(1)–Ru(4)	88.9(1)
Ru(1)–Ir(2)–Ru(3)	88.8(1)	Ru(2)–Ir(2)–Ru(4)	92.3(1)
Ir(1)–Ru(1)–Ir(2)	89.3(1)	Ru(2)–Ru(1)–Ru(4)	89.9(1)
Ir(1)–Ru(2)–Ir(2)	88.7(1)	Ru(1)–Ru(2)–Ru(3)	90.1(1)
Ir(1)–Ru(3)–Ir(2)	89.6(1)	Ru(2)–Ru(3)–Ru(4)	90.0(1)
Ir(1)–Ru(4)–Ir(2)	90.2(1)	Ru(1)–Ru(4)–Ru(3)	89.6(1)
Ir(1)–B–Ir(2)	178.5(18)	Ru(1)–B–Ru(3)	178.7(18)
Ru(2)–B–Ru(4)	174.4(17)		

mutually *trans* indicating that during the transformation from $[Ru_4H(CO)_{12}BH]^-$ to $[Ir_2Ru_4(CO)_{16}B]^-$, the four ruthenium atoms have undergone a rearrangement from a butterfly to square geometry.

The four Ru–Ru edge distances lie in the range 2.934(4)–2.953(3) Å as compared to a range for the Ru–Ir edge distances of 2.870(3)–3.024(3) Å. These values compare with ranges for the Ru–Ru and Ru–Rh edge distances in *trans*-$[Rh_2Ru_4(CO)_{16}B]^-$ of 2.926(2)–2.942(2) and 2.828(2)–3.033(2) Å respectively.*[,4] In anion **2**, the boron atom is fully interstitial with the Ir–B distances being comparable with the Ru–B distances (Table 3). In *trans*-$[Rh_2Ru_4(CO)_{16}B]^-$, the Ru–B and Rh–B distances lie within the range 2.04(1)–2.09(1) Å.[4] Each ruthenium atom in **2** carries three terminal carbonyl ligands and each iridium atom bears two. This situation mimics that observed in the rhodium analogue.[4] However, in **2**, the carbonyl ligand C(15)O(15) [essentially terminally bound to atom Ru(4)] is involved in a semi-bridging interaction to atom Ir(1) [Ru(4)–C(15) 1.91(5), Ir(1)–C(15) 2.42(5) Å and Ru(4)–C(15)–O(15) 147.8(39)°].

Reactions of $[AuCl(PR_3)]$ (R = C_6H_{11}, Ph *or* C_6H_4Me-2) *and Anion* **1**.—The compound $[N(PPh_3)_2][Rh_2Ru_4(CO)_{16}B]$ reacts with $[AuCl\{P(C_6H_{11})_3\}]$ to yield a (≈70% yield) green product, **3a**, and a minor brown product **3b** which converts on standing in CH_2Cl_2 solution to **3a**. A parallel phenomenon occurs when $[AuCl(PPh_3)]$ is used in place of $[AuCl\{P(C_6H_{11})_3\}]$ (Fig. 3). However when the source of gold(I) is $[AuCl\{P(C_6H_4Me\text{-}2)_3\}]$, only a green product results. Compound **3a** has been fully characterized but **3b** could not be obtained pure; spectroscopic data for **3b** were obtained from observations of mixtures of **3a** and **3b**.

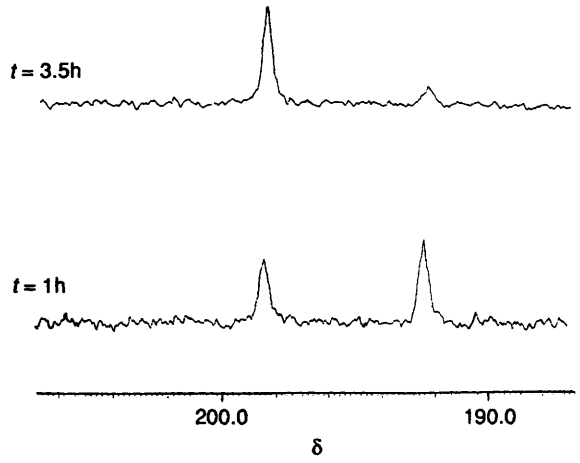

Fig. 3 The 128 MHz ^{11}B NMR spectrum (CD_2Cl_2, 298 K) of a mixture of the green and brown isomers of $[Rh_2Ru_4(CO)_{16}B\{Au(PPh_3)\}]$ showing interconversion from brown to green isomer over a period of a few hours

Green **3a** exhibits a resonance in the ^{11}B NMR spectrum at δ +196.2, close to that observed for the octahedral anion **1a**. Mass spectral data showed an intense envelope at *m/z* 1069 corresponding to cluster **1** in addition to a parent envelope at *m/z* 1549 corresponding to the addition of an $AuP(C_6H_{11})_3$ fragment to **1**. The ^1H and ^{31}P NMR spectral data were also consistent with **3a** being formulated as the monogold(I) phosphine derivative $[Rh_2Ru_4(CO)_{16}B\{AuP(C_6H_{11})_3\}]$. The solution ^{13}C NMR spectrum of **3a** is discussed later. The spectroscopic properties of the green products of the reactions of $[AuCl(PPh_3)]$ and $[AuCl\{P(C_6H_4Me\text{-}2)_3\}]$ and with **1** indicated that these were analogous to **3a**, namely $[Rh_2Ru_4(CO)_{16}B\{Au(PPh_3)\}]$ and $[Rh_2Ru_4(CO)_{16}B\{AuP(C_6H_4Me\text{-}2)_3\}]$.

The molecular structure of **3a** was determined crystallographically (Fig. 4), a suitable crystal being grown from CH_2Cl_2 layered with hexane. Selected bond distances and angles are listed in Table 5. The octahedral core of anionic precursor is retained in the gold(I) phosphine derivative, and the boron atom is fully interstitial with Ru–B and Rh–B distances lying in the range 2.07(2)–2.12(2) Å. As in the structure of anion **1a**,[4] it is not possible to distinguish unambiguously between the ruthenium and rhodium atoms in the M_6 metal core, and carbonyl connectivity data is used to aid their assignment. Of the 16 carbonyl ligands, 12 are terminal and four are edge bridging. It is expected that the connectivity of the ruthenium atoms will be greater than that of the rhodium atoms and that rhodium atoms will be more likely to be associated with the bridging carbonyl ligands than will the ruthenium atoms. Given these criteria, we assign the two rhodium atoms to mutually *trans* positions (Fig. 3) and thus the *trans*-Rh_2Ru_4B core of **1a** is retained when **3a** is formed.

The $AuP(C_6H_{11})_3$ fragment in **3a** caps one face of the Rh_2Ru_4 octahedron; all faces are equivalent (*i.e.*, $RhRu_2$ triangles). This fully μ_3-bonding mode contrasts with the semicapping gold(I) phosphine observed in the related carbido cluster $[Ru_6(CO)_{15}(NO)C\{Au(PPh_3)\}]$.[14,15] The octahedral Rh_2Ru_4 core in **3a** is somewhat distorted with four edges being elongated and four shortened. Three of the longer edges are

* The structure of $[Rh_2Ru_4(CO)_{16}B]^-$ was disordered and data given here refer to the majority structure.

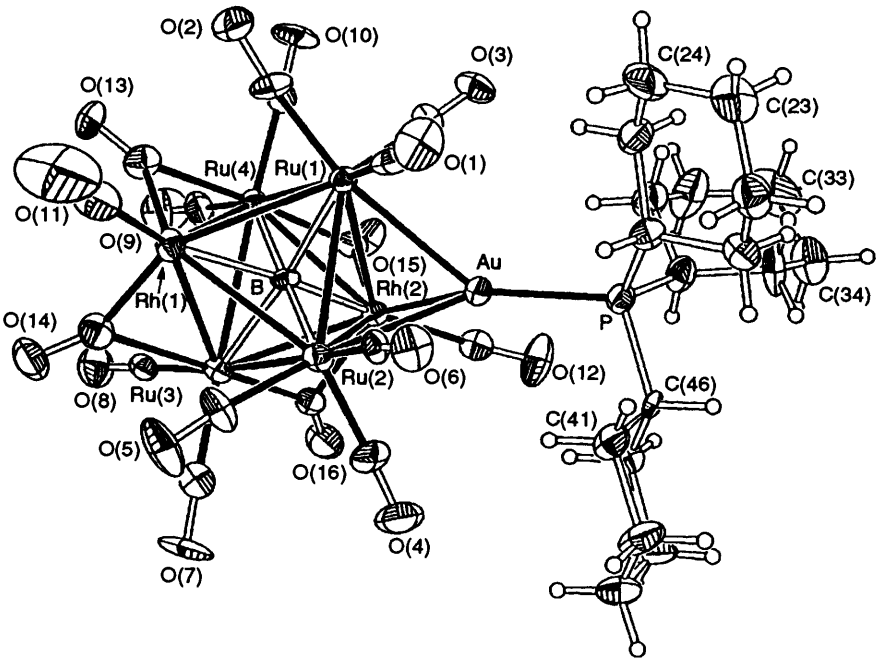

Fig. 4 Molecular structure of $[Rh_2Ru_4(CO)_{16}B\{AuP(C_6H_{11})_3\}]$ **3a**

Table 4 Atomic coordinates ($\times 10^4$) for compound **3a**

Atom	x	y	z	Atom	x	y	z
Au	3 471(1)	7 392(1)	1 054(1)	C(6)	4 238(11)	8 303(9)	2 451(9)
Rh(1)	6 908(1)	7 329(1)	2 175(1)	C(7)	6 652(13)	9 412(10)	945(9)
Rh(2)	4 926(1)	7 462(1)	230(1)	C(8)	7 744(13)	8 191(9)	489(9)
Ru(1)	5 072(1)	6 523(1)	1 765(1)	C(9)	7 405(14)	6 404(11)	234(13)
Ru(2)	5 094(1)	8 275(1)	1 758(1)	C(10)	6 316(13)	5 350(10)	806(8)
Ru(3)	6 600(1)	8 271(1)	892(1)	C(11)	7 427(18)	7 207(12)	3 209(10)
Ru(4)	6 477(1)	6 486(1)	813(1)	C(12)	3 766(12)	7 579(10)	−508(8)
P	1 838(3)	7 364(3)	843(2)	C(13)	7 584(14)	6 390(10)	1 799(10)
B	5 775(12)	7 393(9)	1 284(9)	C(14)	7 759(14)	8 170(11)	1 998(10)
O(1)	3 882(13)	6 562(10)	2 990(9)	C(15)	5 483(13)	6 604(9)	−271(10)
O(2)	6 323(10)	5 295(8)	2 696(8)	C(16)	5 733(13)	8 331(9)	−177(10)
O(3)	3 848(10)	5 257(7)	840(7)	C(21)	454(13)	7 133(11)	1 775(11)
O(4)	4 166(12)	9 610(7)	751(8)	C(22)	343(15)	6 853(11)	2 540(11)
O(5)	6 412(11)	9 400(9)	2 757(8)	C(23)	610(15)	6 031(13)	2 710(11)
O(6)	3 727(10)	8 385(8)	2 830(7)	C(24)	1 577(15)	5 818(12)	2 576(11)
O(7)	6 668(12)	10 085(7)	955(8)	C(25)	1 726(14)	6 075(10)	1 820(10)
O(8)	8 453(11)	8 185(9)	352(8)	C(26)	1 503(12)	6 959(9)	1 667(9)
O(9)	8 004(13)	6 338(10)	−76(10)	C(31)	1 752(15)	6 085(10)	−159(11)
O(10)	6 231(11)	4 699(6)	820(8)	C(32)	1 364(15)	5 782(14)	−934(12)
O(11)	7 641(22)	7 147(12)	3 819(10)	C(33)	341(20)	5 709(14)	−1 101(13)
O(12)	3 053(9)	7 627(10)	−910(7)	C(34)	−165(15)	6 454(12)	−960(10)
O(13)	8 254(9)	6 023(8)	1 980(8)	C(35)	205(12)	6 763(13)	−153(11)
O(14)	8 433(11)	8 521(8)	2 207(8)	C(36)	1 280(13)	6 872(10)	−36(10)
O(15)	5 459(9)	6 359(7)	−856(6)	C(41)	1 692(13)	8 875(10)	1 448(9)
O(16)	5 659(11)	8 642(8)	−747(8)	C(42)	1 267(15)	9 717(10)	1 351(11)
C(1)	4 292(18)	6 575(10)	2 527(12)	C(43)	1 541(16)	10 122(11)	684(13)
C(2)	5 886(14)	5 792(10)	2 359(9)	C(44)	1 272(16)	9 659(9)	9(11)
C(3)	4 300(12)	5 732(10)	1 189(8)	C(45)	1 659(13)	8 800(9)	93(10)
C(4)	4 512(14)	9 096(11)	1 127(11)	C(46)	1 369(10)	8 365(8)	745(9)
C(5)	5 959(14)	8 952(11)	2 394(11)				

associated with the presence of the capping gold fragment and in particular Ru(1)–Rh(2) is 3.201(2) Å. The four edges bridged by carbonyl ligands suffer consequential shortening [av. 2.818(1) Å].

In solution ($CDCl_3$) at 298 K, the ^{13}C NMR spectrum of **3a** exhibits a triplet resonance in the carbonyl region (δ +200.4) which begins to collapse at 185 K (CD_2Cl_2). The triplet nature (J = 11 Hz) of the signal is attributed to ^{103}Rh–^{13}C spin–spin coupling and indicates that the 16 carbonyl ligands are fluxional. A similar situation has been observed in the octahedral carbide cluster $[Ru_3Rh_3(CO)_{15}C]^-$ for which a quartet (J_{RhC} = 12 Hz) is observed in the ^{13}C NMR spectrum at room temperature in the carbonyl region; this signal begins to broaden at 183 K.[16] However, in the case of **3a**, the solid-state structure indicates that the two rhodium atoms are not equivalent. It may of course be possible that the triplet comprises two doublets with coincident coupling constants. Alternatively, the fluxional process of the carbonyl ligands may be accompanied by a rocking motion of the $AuP(C_6H_{11})_3$ fragment (Fig. 5) which would render the two rhodium nuclei

Table 5 Selected bond distances (Å) and angles (°) for compound **3a**

Rh(1)–Ru(1)	2.941(2)	Rh(1)–Ru(2)	3.032(2)
Rh(1)–Ru(3)	2.800(2)	Rh(1)–Ru(4)	2.834(2)
Rh(2)–Ru(1)	3.201(2)	Rh(2)–Ru(2)	3.088(2)
Rh(2)–Ru(3)	2.828(2)	Rh(2)–Ru(4)	2.811(2)
Ru(1)–Ru(2)	2.951(2)	Ru(2)–Ru(3)	2.952(2)
Ru(3)–Ru(4)	3.014(2)	Ru(1)–Ru(4)	2.944(2)
Ru(1)–B	2.08(2)	Ru(2)–B	2.07(2)
Ru(3)–B	2.12(2)	Ru(4)–B	2.12(1)
Rh(1)–B	2.07(2)	Rh(2)–B	2.07(2)
Au–Rh(2)	2.838(2)	Au–Ru(1)	2.825(2)
Au–Ru(2)	2.857(2)	Au–P	2.316(4)
Rh(2)–Au–Ru(1)	68.9(1)	Rh(2)–Au–Ru(2)	65.7(1)
Rh(1)–Au–Ru(2)	62.6(1)	Rh(2)–Au–P	139.1(1)
Ru(1)–Au–P	141.2(1)	Ru(2)–Au–P	143.4(1)
Ru(1)–Rh(1)–Ru(3)	93.8(1)	Ru(2)–Rh(1)–Ru(4)	91.1(1)
Ru(2)–Rh(2)–Ru(4)	90.4(1)	Ru(1)–Rh(2)–Ru(3)	87.9(1)
Ru(2)–Ru(1)–Ru(4)	90.5(1)	Rh(1)–Ru(1)–Rh(2)	83.7(1)
Rh(1)–Ru(2)–Rh(2)	84.2(1)	Ru(1)–Ru(2)–Ru(3)	90.6(1)
Rh(1)–Ru(3)–Rh(2)	93.6(1)	Ru(2)–Ru(3)–Ru(4)	89.2(1)
Rh(1)–Ru(4)–Rh(2)	93.2(1)	Ru(1)–Ru(4)–Ru(3)	89.5(1)
Rh(1)–B–Rh(2)	164.6(10)	Ru(1)–B–Ru(3)	174.2(8)
Ru(2)–B–Ru(4)	179.3(9)		

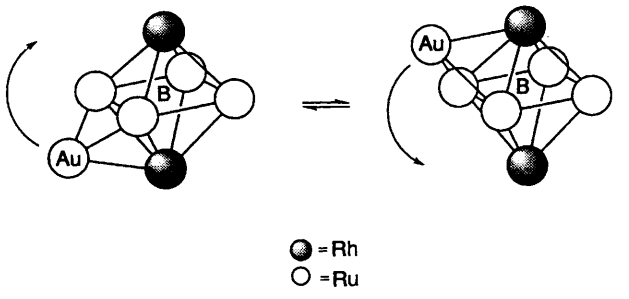

Fig. 5 The proposed fluxional process for *trans*-$[Rh_2Ru_4(CO)_{16}B\{AuP(C_6H_{11})_3\}]$ **3a** which renders the two rhodium centres in the Rh_2Ru_4 core equivalent

equivalent. We have proposed a similar rocking motion in the related trigold system $[Ru_6(CO)_{16}B\{Au(PPh_3)\}_3]$ to account for equivalence in two of the three phosphorus environments.[3] Fluxional processes involving cluster-bound Group 11 fragments in Au_2Ru_4 cores have been discussed by Orpen and Salter.[17]

Compound **3b** is an isomer of **3a** and we propose that the two isomers bear the same relationship to one another as do **1b** and **1a** (Fig. 6). The ^{11}B NMR spectrum of a mixture of **3a** and **3b** shows a triplet at δ +192.0 (J_{RhB} = 22 Hz) in addition to the resonance at δ +196.2 assigned to **3a**. Note that for **3a**, no coupling between the ^{103}Rh and ^{11}B nuclei could be resolved, but for **3b**, the triplet confirms the presence of the two cage rhodium atoms. The mass spectrum of a mixture of **3a** and **3b** shows no other features than those attributed to **3a**, thereby supporting the suggestion that **3a** and **3b** are isomers. The IR spectrum of **3a** exhibits absorptions due to both terminal and bridging carbonyl stretching modes. For a mixture of **3a** and **3b**, an additional absorption at 2039 cm^{-1} was observed. Similar relationships are observed between the green and brown products of the reaction of $[AuCl(PPh_3)]$ and **1** as between compounds **3a** and **3b**, indicating that in each case an analogous pair of isomers is formed. The conversion of the brown to the green isomer may be monitored by using ^{11}B NMR spectroscopy and this is shown for $[Rh_2Ru_4(CO)_{16}B\{Au(PPh_3)\}]$ in Fig. 3.

With the confirmation that compound **3a** may be formulated as *trans*-$[Rh_2Ru_4(CO)_{16}B\{AuP(C_6H_{11})_3\}]$, it is reasonable to assign analogous structures to the green products of the reactions of $[AuCl(PPh_3)]$ and $[AuCl\{P(C_6H_4Me\text{-}2)_3\}]$ with **1**.

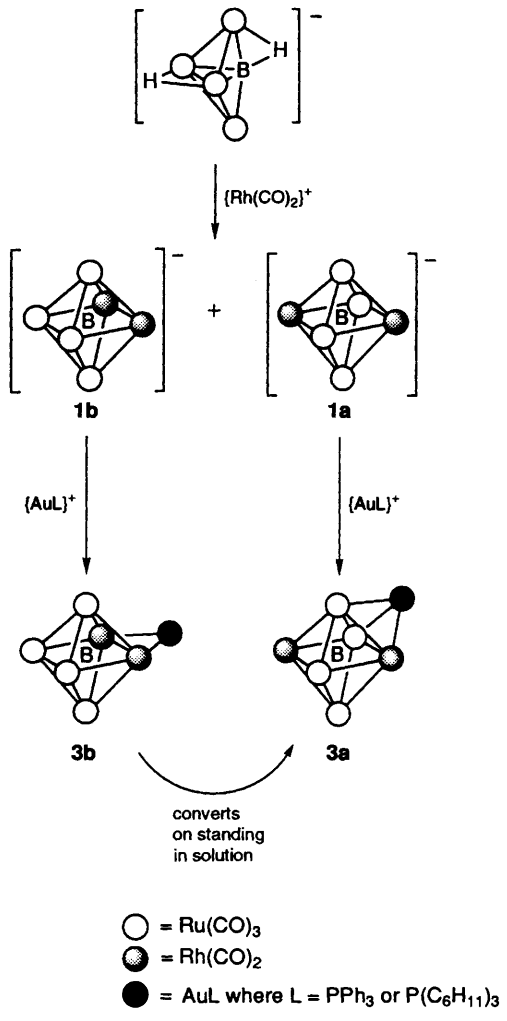

Fig. 6 Schematic representation of the formation of anions **1a** and **1b** followed by their reactions with gold(I) phosphine fragments to give **3a** and **3b**. The edge-bridging site for the gold atom in **3b** is modelled on that found for the iridium analogue, **4**

The IR spectral signatures of the three green products are all similar. We propose that **3b** and the brown product from the reaction of **1** with $[AuCl(PPh_3)]$ are the *cis* analogues of **3a** and its triphenylphosphine counterpart. It seems reasonable that a pathway as illustrated in Fig. 6 operates and we have spectroscopic or crystallographic evidence for each species in the sequence of reactions. Further evidence for the *cis* arrangement of Group 9 metal atoms comes from a study of the reaction of anion **2** with gold(I) phosphines.

Reactions of $[AuCl(PR_3)]$ (R = C_6H_{11} *or* Ph) *and Anion* **2**.—In anion **2** the iridium atoms are in a *trans* arrangement. Its $[N(PPh_3)_2]^+$ salt reacts smoothly with either $[AuCl(PPh_3)]$ or $[AuCl\{P(C_6H_{11})_3\}]$ to give a neutral product in each case. Mass spectral data support the addition of one $\{Au(PPh_3)\}$ or $\{AuP(C_6H_{11})_3\}$ unit to anion **2**. The ^{11}B NMR spectra of the two products both show resonances close to δ +199. The IR spectral signatures of the two products are similar but are *unlike* those of **3a** and its congeners. In order to elucidate the exact nature of these products, we undertook a crystal structure study of $[Ir_2Ru_4(CO)_{16}B\{AuP(C_6H_{11})_3\}]$ **4**.

A crystal of **4** of X-ray quality was grown from CH_2Cl_2 layered with hexane. Its molecular structure is shown in Fig. 7 and selected bond distances and angles are listed in Table 7. Neutral **4** possesses an octahedral Ir_2Ru_4 core with the two iridium atoms in *cis* positions. This is in contrast to the *trans*

Table 6 Atomic coordinates ($\times 10^4$) for compound **4**

Atom	*x*	*y*	*z*	Atom	*x*	*y*	*z*
Au	5 000	7 612(1)	5 000	C(6)	4 670(14)	6 581(33)	6 808(19)
Ir(1)	4 148.6(7)	9 074(1)	5 431(1)	C(7)	3 834(14)	4 831(38)	6 687(21)
Ir(2)	4 221.3(7)	5 798(1)	4 907(1)	C(8)	3 076(17)	9 351(42)	3 661(25)
Ru(1)	3 976(1)	6 668(3)	6 329(2)	C(9)	3 301(17)	6 390(45)	3 275(25)
Ru(2)	3 533(1)	7 793(3)	4 054(2)	C(10)	4 001(13)	8 393(34)	3 493(19)
Ru(3)	3 117(1)	8 462(3)	5 500(2)	C(11)	2 700(17)	7 934(42)	6 244(24)
Ru(4)	3 144(1)	5 668(3)	5 012(2)	C(12)	2 515(19)	9 303(45)	4 983(27)
P	5 785(3)	8 461(8)	4 930(4)	C(13)	3 511(20)	10 176(58)	5 980(30)
B	3 753(27)	7 235(41)	5 226(22)	C(14)	3 294(19)	3 950(52)	4 491(29)
O(1)	4 883(11)	10 161(39)	6 855(16)	C(15)	2 433(24)	6 330(65)	4 439(36)
O(2)	4 346(11)	11 546(30)	4 449(21)	C(16)	2 828(19)	4 630(47)	5 685(28)
O(3)	4 906(15)	3 630(34)	5 841(20)	C(21)	6 369(13)	6 414(33)	5 907(19)
O(4)	4 475(12)	4 916(34)	3 400(14)	C(22)	6 711(24)	6 177(68)	6 652(36)
O(5)	3 720(15)	8 223(38)	7 711(15)	C(23)	6 589(17)	6 711(40)	7 334(23)
O(6)	5 036(12)	6 616(41)	7 122(19)	C(24)	6 485(14)	8 210(36)	7 267(21)
O(7)	3 813(16)	3 706(31)	6 921(17)	C(25)	6 096(13)	8 513(34)	6 550(19)
O(8)	2 815(14)	10 224(51)	3 343(22)	C(26)	6 247(13)	8 043(31)	5 807(18)
O(9)	3 122(22)	5 642(39)	2 816(17)	C(31)	5 488(16)	10 930(37)	4 079(23)
O(10)	4 316(14)	8 757(38)	3 156(16)	C(32)	5 365(16)	12 481(37)	4 158(24)
O(11)	2 500(15)	7 742(47)	6 687(22)	C(33)	5 868(21)	13 204(59)	4 354(33)
O(12)	2 180(11)	9 904(46)	4 615(24)	C(34)	6 175(21)	12 855(47)	5 241(29)
O(13)	3 520(14)	11 235(44)	6 258(44)	C(35)	6 284(16)	11 143(43)	5 187(26)
O(14)	3 318(13)	2 941(42)	4 247(34)	C(36)	5 769(14)	10 422(36)	4 893(21)
O(15)	2 114(10)	6 455(43)	3 991(21)	C(41)	6 522(14)	8 257(36)	3 929(20)
O(16)	2 603(22)	4 165(43)	6 098(21)	C(42)	6 745(18)	7 591(41)	3 286(25)
C(1)	4 631(15)	9 653(37)	6 273(22)	C(43)	6 283(17)	7 469(43)	2 587(25)
C(2)	4 226(17)	10 558(43)	4 785(24)	C(44)	5 773(15)	6 852(41)	2 726(23)
C(3)	4 617(12)	4 413(30)	5 482(17)	C(45)	5 603(14)	7 569(35)	3 381(19)
C(4)	4 403(12)	5 271(32)	3 944(19)	C(46)	5 998(12)	7 728(30)	4 121(17)
C(5)	3 805(17)	7 622(40)	7 193(25)	O(100)	7 492(15)	7 539(30)	7 517(21)

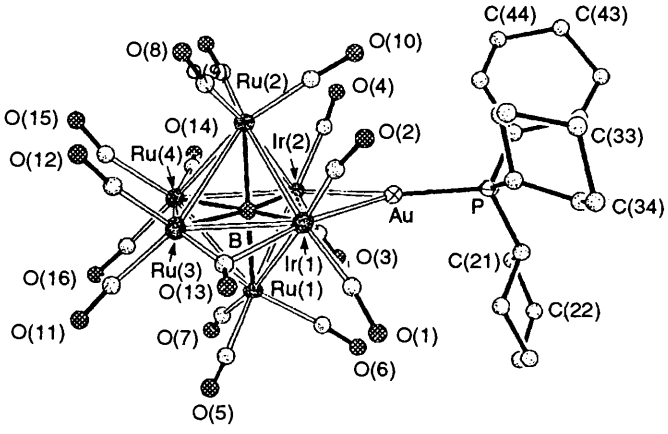

Fig. 7 Molecular structure of $[Ir_2Ru_4(CO)_{16}B\{AuP(C_6H_{11})_3\}]$ **4**

Table 7 Selected bond distances (Å) and angles (°) for compound **4**

Ir(1)–Ru(1)	2.879(4)	Ir(1)–Ru(2)	2.915(4)
Ir(1)–Ru(3)	2.857(4)	Ir(1)–Ir(2)	3.273(2)
Ir(2)–Ru(1)	2.851(4)	Ir(2)–Ru(2)	2.855(3)
Ir(2)–Ru(4)	2.941(4)	Ru(1)–Ru(3)	2.999(4)
Ru(1)–Ru(4)	3.030(4)	Ru(2)–Ru(4)	2.965(5)
Ru(3)–Ru(4)	2.803(4)	Ru(2)–Ru(3)	3.062(5)
Ru(1)–B	1.99(4)	Ru(2)–B	2.10(4)
Ru(3)–B	2.20(6)	Ru(4)–B	2.19(6)
Ir(1)–B	2.04(5)	Ir(2)–B	2.02(6)
Au–Ir(1)	2.910(2)	Au–Ir(2)	2.691(2)
Au–P	2.285(8)		
Ir(1)–Au–Ir(2)	71.4(1)	Ir(1)–Au–P	128.9(2)
Ir(2)–Au–P	159.7(2)	Au–Ir(1)–Ru(1)	89.3(1)
Au–Ir(1)–Ru(2)	85.5(1)	Au–Ir(1)–Ru(3)	137.2(1)
Au–Ir(2)–Ru(1)	94.4(1)	Au–Ir(2)–Ru(2)	90.9(1)
Au–Ir(2)–Ru(4)	141.8(1)	Ru(1)–Ir(1)–Ru(2)	90.0(1)
Ru(1)–Ir(2)–Ru(2)	91.8(1)	Ir(2)–Ru(1)–Ru(3)	91.6(1)
Ir(1)–Ru(1)–Ru(4)	90.2(1)	Ir(2)–Ru(2)–Ru(3)	90.3(1)
Ir(1)–Ru(2)–Ru(4)	90.8(1)	Ru(1)–Ru(3)–Ru(2)	85.0(1)
Ir(1)–Ru(3)–Ru(4)	95.4(1)	Ru(1)–Ru(4)–Ru(2)	86.2(1)
Ir(2)–Ru(4)–Ru(3)	93.9(1)	Ir(1)–Ir(2)–Ru(4)	84.6(1)
Ir(2)–Ir(1)–Ru(3)	86.1(1)	Ru(1)–B–Ru(2)	178(4)
Ir(2)–B–Ru(3)	168(3)	Ir(1)–B–Ir(4)	164(3)

sites noted in the structure of **2** and the *trans* sites observed for the rhodium atoms in **3a**.

The gold atom in **4** bridges the Ir–Ir edge and this interaction causes elongation of the Ir–Ir distance to 3.273(2) Å. However, in order for **4** to possess an electron count which is consistent with the accepted number assigned to an octahedral structure (*i.e.* 86), the Ir–Ir interaction should be considered to be a bonding one. With respect to the plane containing the atoms Ru(4), Ru(3), Ir(1) and Ir(2), the gold atom is raised 0.15 Å and the phosphorus atom, 0.31 Å. The maximum deviation of the boron atom from this plane is 0.04 Å.

The boron atom is fully interstitial but is displaced towards the two iridium atoms. This is apparent if the metal–boron distances within the equatorial plane containing the boron and gold atoms are examined: Ru(3)–B 2.20(6), Ru(4)–B 2.19(6), Ir(1)–B 2.04(5) and Ir(2)–B 2.02(6) Å.

Each ruthenium atom bears three terminal carbonyl ligands and each iridium atom carries two. The only exception is that carbonyl C(13)O(13) is semi-bridging between atoms Ru(3) and Ir(1) but remains essentially terminally bound to atom Ru(3) [Ru(3)–C(13) 2.03(5), Ir(1)–C(13) 2.38(6) Å and Ru(3)–C(13)–O(13) 150.3(48)°].

Conclusion

The determinations of the solid-state structures of **2** and **4** carry with them the message that the attachment of the gold(I) phosphine fragment does not appear to be a straightforward addition. That the gold(I) fragment prefers to be associated with two adjacent iridium (rather than two ruthenium, or one

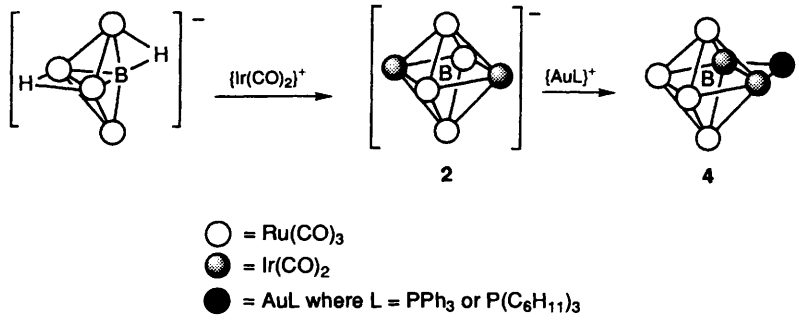

Fig. 8 Schematic representation of the formation of anion **2** followed by its reaction with gold(I) phosphine fragments to give **4**

ruthenium and one iridium) atoms is consistent with a consideration of bond energetics and it brings to the fore the question of skeletal isomerism. If only the crystal structure data are considered, then we have the scenario that the Ir_2Ru_4B core undergoes a *cis* ⟶ *trans* isomerisation when **2** is formed and then a *trans* ⟶ *cis* rearrangement on going from **2** to **4** (Fig. 8). This scenario is reasonable in terms of metal–metal bond energetics and the presence of the interstitial boron atom presumably helps to stabilize the system as isomerization occurs. On the other hand, we cannot rule out the possibility that in solution anion **2** consists of a mixture of the *cis*- and *trans*-skeletal isomers. However, whereas we have NMR spectral evidence for this being the case for the rhodium congener, **1**, we have no such evidence for it being true for **2**.

Acknowledgements

We thank the donors of the Petroleum Research Fund, administered by the American Chemical Society, for support of this work (grant #25533-AC3), the SERC for studentships (to J. R. G., A. W. and A. D. H.) and the National Science Foundation for a grant (CHE 9007852) towards the purchase of a diffractometer at the University of Delaware.

References

1 S. M. Draper, C. E. Housecroft, A. K. Keep, D. M. Matthews, X. Song and A. L. Rheingold, *J. Organomet. Chem.*, 1992, **423**, 241.
2 C. E. Housecroft, D. M. Matthews, A. L. Rheingold and X. Song, *J. Chem. Soc., Chem. Commun.*, 1992, 842.
3 C. E. Housecroft, D. M. Matthews, A. Waller, A. J. Edwards and A. L. Rheingold, *J. Chem. Soc., Dalton Trans.*, 1993, 3059.
4 J. R. Galsworthy, C. E. Housecroft and A. L. Rheingold, *J. Chem. Soc., Dalton Trans.*, 1994, 2359.
5 F.-E. Hong, T. J. Coffy, D. A. McCarthy and S. G. Shore, *Inorg. Chem.*, 1989, **28**, 3284.
6 R. Khattar, J. Puga, T. P. Fehlner and A. L. Rheingold, *J. Am. Chem. Soc.*, 1989, **111**, 1877.
7 A. K. Bandyopadhyay, R. Khattar and T. P. Fehlner, *Inorg. Chem.*, 1989, **28**, 4434.
8 A. K. Bandyopadhyay, R. Khattar, J. Puga, T. P. Fehlner and A. L. Rheingold, *Inorg. Chem.*, 1992, **31**, 465.
9 A. D. Hattersley, Ph.D. Thesis, University of Cambridge, 1993.
10 A. K. Chipperfield, C. E. Housecroft and A. L. Rheingold, *Organometallics*, 1990, **9**, 681.
11 F.-E. Hong, D. A. McCarthy, J. P. White, C. E. Cottrell and S. G. Shore, *Inorg. Chem.*, 1990, **29**, 2874.
12 C. R. Eady, B. F. G. Johnson and J. Lewis, *J. Chem. Soc., Dalton Trans.*, 1977, 477.
13 G. Sheldrick, SHELXTL-PC software version 4.2, Siemens XRD, Madison, WI, 1991.
14 B. F. G. Johnson, J. Lewis, W. J. H. Nelson, J. Puga, P. R. Raithby, D. Braga, M. McPartlin and W. Clegg, *J. Organomet. Chem.*, 1983, **243**, C13.
15 B. F. G. Johnson, J. Lewis, W. J. H. Nelson, J. Puga, M. McPartlin and A. Sironi, *J. Organomet. Chem.*, 1983, **253**, C5.
16 M. P. Jensen, W. Henderson, D. H. Johnston, M. Sabat and D. F. Shriver, *J. Organomet. Chem.*, 1990, **394**, 121.
17 A. G. Orpen and I. D. Salter, *Organometallics*, 1991, **10**, 111.

Received 2nd September 1994; *Paper* 4/05361C